Thermodynamically Stable Phases of Carbon at Multiterapascal Pressures

Miguel Martinez-Canales* and Chris J. Pickard
Department of Physics & Astronomy, University College London, Gower Street, London WC1E 6BT, United Kingdom
Richard J. Needs
Theory of Condensed Matter Group, Cavendish Laboratory, Cambridge CB3 0HE, United Kingdom
(Received 16 May 2011; published 26 January 2012)

Phases of carbon are studied up to pressures of 1 petapascal (PPa) using first-principles density-functional-theory methods and a structure searching algorithm. Our extensive search over the potential energy surface supports the sequence of transitions diamond → BC8 → simple cubic under increasing pressure found in previous theoretical studies. At higher pressures we predict a soft-phonon driven transition to a simple hexagonal structure at 6.4 terapascals (TPa), and further transitions to the face centered cubic electride structure at 21 TPa, a double hexagonal close packed structure at 270 TPa, and the body centered cubic structure at 650 TPa.

DOI: 10.1103/PhysRevLett.108.045704 PACS numbers: 64.70.K−, 61.50.Ks, 62.50.−p, 71.15.Mb

Carbon is the fourth most abundant element in the Universe [1] and it exhibits a rich variety of allotropes, such as diamond, graphite, and fullerenes, to name but a few. Graphite is the most stable allotrope under ambient conditions, but the much denser diamond phase is stable from moderate pressures up to roughly 1 TPa, which is about 3 times the pressure at the center of Earth. Knowledge of the phase diagram of carbon at high pressures and temperatures is important for understanding the equations of state of astrophysical bodies such as solar and extrasolar planets [2] and white dwarf stars [3]. Exoplanets with carbon-rich interiors have been postulated [4]. The atmosphere of the exoplanet Wasp-12b has a very high carbon-oxygen ratio and it might have a carbon dominated interior [5]. The carbon-rich cores of cooling white dwarf stars, such as BPM 37093, could crystallize from the center outwards [3]. Exploring the phase diagram of carbon under extreme conditions using shock-wave [6,7] and ramped-compression experiments [8] is a very active area of research. High-density carbon is also a candidate ignition capsule ablator material for inertial confinement fusion experiments such as those underway at the National Ignition Facility [9].

Information about the equation of state of diamond at high pressures has been obtained from static compression experiments using diamond anvil cells [10] which have reached pressures of 0.41 TPa [11]. Ramped-compression experiments have shown that the solid diamond phase is stable up to at least 0.8 TPa [8]. The melting of carbon at high pressures and temperatures has been studied in shock-wave experiments [6,7], and Knudson *et al.* have found evidence for a second solid phase [6]. This is consistent with the prediction from density-functional-theory (DFT) calculations that diamond transforms to the BC8 structure at around 1 TPa [12–14]. DFT calculations predict a further transition to the simple cubic (sc) structure at about 3 TPa [12–15], but we are not aware of any predictions of phase transitions at higher pressures.

Diamond is an insulator with perfect tetrahedral sp^3 bonding. The BC8 phase also has sp^3 bonding, but some of its bond angles are distorted. The resulting structure is denser than diamond and has a much reduced band gap, becoming weakly metallic within DFT under pressure. The strong covalent bonding is lost at the transition from BC8 to the sixfold coordinated and metallic sc structure. The progression from four- to six-fold structures suggests a steady increase in coordination number towards close packed phases, which are presumably the most favorable at extremely high pressures. However, experiments have shown that the alkali metals, which adopt the body centered cubic structure (bcc) at ambient conditions, transform to more open structures at higher pressures [16]. In addition, DFT calculations have shown that aluminum (Al), which adopts the face centered cubic structure (fcc) at ambient conditions, transforms to open phases at multi-TPa pressures [17]. The alkalis and Al therefore show a reduction in coordination number with increasing pressure.

We emphasize that there is no direct experimental evidence for the stability of BC8 carbon at high pressures, and no experimental evidence whatsoever for the stability of sc carbon. There is, however, every reason to believe that carbon will undergo further structural phase transitions with increasing pressure. We have performed a computational search for carbon structures to explore these issues using the *ab initio* random structure searching (AIRSS) approach [18,19], in which randomly chosen structures are relaxed to a minimum in the enthalpy. We have often used AIRSS with constraints on the crystal symmetry or using experimental information [19], but in this study we have used the ''primitive'' unconstrained AIRSS method which is unbiased and allows any structure to be formed. AIRSS has already been applied successfully to systems under

extreme conditions such as hydrogen [20], lithium [21], Al [17], and iron [22].

We used the CASTEP [23] plane-wave basis set DFT code and the Perdew-Burke-Ernzerhof (PBE) [24] Generalized Gradient Approximation (GGA) density functional. Searches were performed at 1, 1.5, 2, 4, 10, 25, 50, 100, 300, and 1000 TPa (= 1 PPa). The searches encompassed structures with 2, 4, 6, 8, 10, and 12 atoms per unit cell (the latter only between 4 and 100 TPa), but we also performed searches at 10 and 25 TPa with 5, 7, 9, and 11 atoms. For each pressure and number of atoms, random structures were generated and relaxed until the lowest enthalpy structure was found several times. Above 10 TPa we found that the energy landscape simplifies and a large fraction of the random structures relax to the most stable structure, even with 10 or more atoms. In total, more than 7000 structures were relaxed.

To approach all-electron accuracy we used ultrasoft pseudopotentials [25] treating all six electrons explicitly. At pressures above 300 TPa we used a pseudopotential with a very small core radius of 0.6 a.u. to obtain converged energy differences between the phases. Such a pseudopotential is, however, very inefficient at lower pressures because the large volumes per atom require much larger basis sets, and to reduce the computational cost we used pseudopotentials with larger core radii at lower pressures [26]. Between 50 and 300 TPa we used a pseudopotential with a core radius of 0.8 a.u. and below 25 TPa we used one with a core radius of 1 a.u. Using different pseudopotentials creates discontinuities in the enthalpy curves at 50 and 300 TPa, but they are only a few meV per atom and cannot be resolved in Fig. 1. The highest pressure transition that we have found is between the double hexagonal close packed (dhcp) and bcc structures at 650 TPa (see below). We also calculated the pressure of this transition using the bare $-6/r$ Coulomb nuclear potential with plane wave cutoff energies up to 35 keV, obtaining a transition pressure of 656 TPa, which differs from our pseudopotential result by about 1%. Details of the basis set cutoffs and Brillouin zone integration grids are given in the supplemental material [27]. Given that PBE-DFT has not been tested at such extreme pressures, we have included a discussion of the accuracy of this approach in the supplemental material [27].

The relative enthalpies of the most stable structures over the pressure range 0.8–1000 TPa are shown in Fig. 1. Our results agree with the sequence of phase transitions diamond → BC8 → sc reported previously [12–14], and support this sequence because we have explored structures corresponding to many different local minima in the energy landscape. We find pressures of 0.99 TPa for the diamond → BC8 and 2.9 TPa for BC8 → sc transitions, which are in good agreement with previous theoretical values [12–14]. At higher pressures we find the sequence sc → sh → fcc → dhcp → bcc, with transition pressures of 6.4, 21, 270, and 650 TPa, where sh denotes the simple hexagonal structure.

A deformation of the sc phase with *Pmma* symmetry is almost degenerate with sc in the range 3–6 TPa. To establish which phase is stable, the phonon spectrum of sc carbon was computed at several pressures (see Fig. 2). The transverse phonon at *X*, corresponding to the *Pmma* distortion, is very soft, and the band structure indicates that a Peierls distortion might take place. Computing the energy along the phonon displacement reveals two local minima separated by ~0.05 Å, with an energy barrier of 1 ~ meV per atom. As a result, we expect the vibrationally averaged structure to be sc. Above 6.4 TPa, however, the *Pmma* structure can immediately deform to sh carbon. Note that as the pressure is decreased to 2 TPa the transverse acoustic branches of the sc phase become unstable at the *R* point,

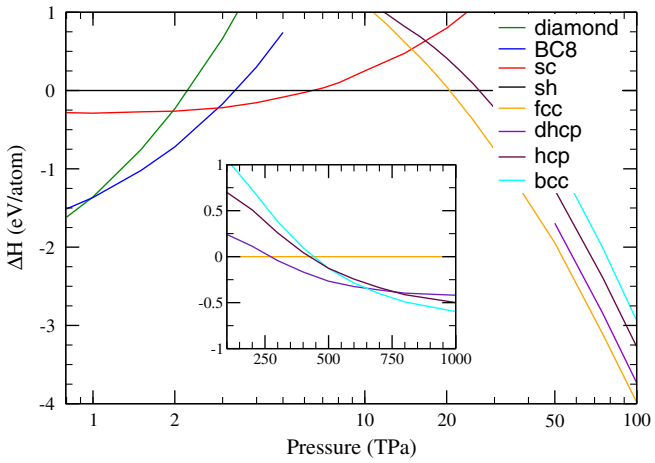

FIG. 1 (color online). Variation of the enthalpies of the phases with pressure. The enthalpy of sh carbon is taken as reference in the main graph while the fcc structure is the reference for the inset showing the ultrahigh pressure regime.

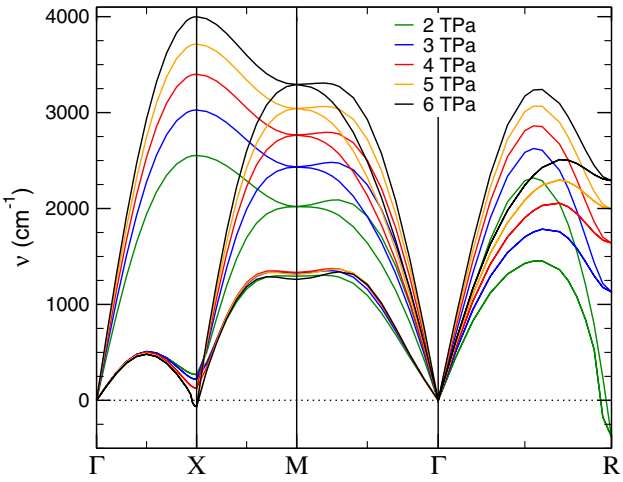

FIG. 2 (color online). Evolution of the phonon dispersion relations of sc carbon with pressure. As the pressure is increased the acoustic phonon branch becomes unstable at *X* and a phase transition to the sh structure occurs.

showing that sc carbon is dynamically unstable at lower pressures. Stabilizing this distortion requires a unit cell with at least 8 atoms, which is consistent with metadynamics calculations that recover BC8 carbon from sc on pressure release [28].

Phonon calculations over a wide range of pressures show that all the newly proposed phases are dynamically stable, see the supplemental material [27]. Including the zero point enthalpy reduces the BC8 → sc transition pressure to 2.5 TPa, the sc → sh transition to 4.8 TPa and the sh → fcc transition to 19 TPa. The stable structures at higher pressures are all close packed and have almost identical zero point enthalpies, so that the transition pressures are unaffected. The computed vibrational data allow us to extend our results to finite temperature using the quasiharmonic approximation. Combining these results with the data for BC8 from Ref. [29] and the Lindemann melting criterion [27] for the higher pressure phases we arrive at the phase diagram shown in Fig. 3. Note that the sc phase is not stable above 5000 K, which explains why it has not been found in molecular dynamics simulations. The quasiharmonic approximation is expected to be accurate if the thermal expansivity reaches a well-defined plateau after the initial rise at low temperatures [30]. Fig. 9 of the supplemental material [27] shows the thermal expansivity as a function of temperature and pressure for the sh and fcc phases. This graph suggests that the quasiharmonic approximation is accurate in the sh phase, although it must fail as the melting temperature is approached, and that while it may not be accurate in the lower-pressure portion of the stability region of fcc carbon, it is likely to be accurate up to 12 000 K at pressures of 50 TPa and above.

There has been much recent discussion of the formation of electridelike structures in sp bonded elements at high pressures, in which the interstitial electrons form the anions. [21,31–33]. Designating a phase as an electride is a qualitative judgement about its electronic structure. We designate a carbon phase as an electride if its $2s/2p$-derived charge density and electron localization function (ELF) have well-developed maxima which are well away from the ions and the C–C "*bonds*". Under this definition the sh and lower-pressure phases are not electrides, but the fcc phase is clearly an electride. The ELF of fcc carbon at 25 TPa is illustrated in Fig. 4. The carbon atoms occupy the $4a$ Wyckoff orbit of the fcc lattice. The maxima of the $2s/2p$-derived charge density and the ELF coincide and there are two interstitial maxima per atom centered on the octahedrally coordinated $8c$ orbit. The $2s/2p$-derived valence band is rather flat, which is consistent with the observed localization of the charge density [27]. This phase can therefore be described as an ionic crystal with the carbon ions as the cations and the interstitial electron maxima the anions. The fcc phase can be viewed as forming the CaF_2 ionic structure with Ca atoms replacing the carbon nuclei and F atoms replacing the interstitial electron maxima. The distribution of the valence charge density in the dhcp structure shown in Fig. 11 of the supplemental material [27] is complex and it might best be described as a weak electride. The bcc phase is not an electride as its $2s/2p$ valence charge density is fairly uniform, which gives a low kinetic energy, and bcc is then the most favorable structure as it has the lowest electrostatic energy or, equivalently, the largest Madelung constant. Note that the total charge density of the bcc phase at 1 PPa is far from uniform because the $1s$ orbitals are still strongly localized (see Fig. 5 of the supplemental material [27]), and further phase transitions could occur at even greater pressures.

The c/a ratio of the dhcp phase of 3.28 is very close to the ideal value of 3.266. The carbon dhcp structure has 12

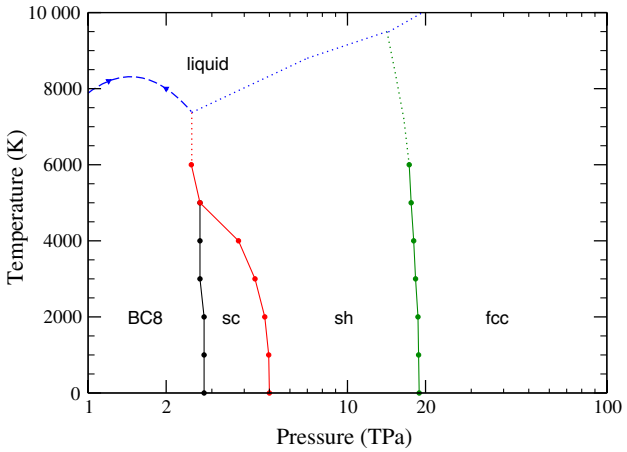

FIG. 3 (color online). Phase diagram of carbon. The solid lines were obtained from our static lattice DFT and vibrational data while the dashed line shows results from molecular dynamics simulations [29]. The dotted lines are estimates based on the DFT data and the Lindemann criterion.

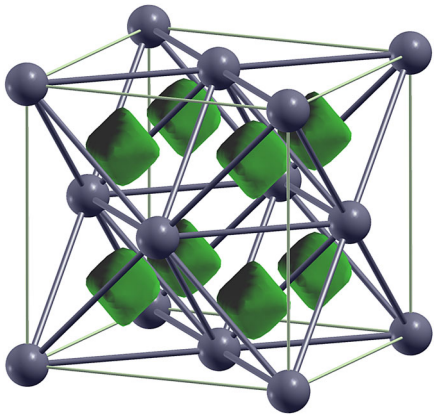

FIG. 4 (color online). Crystal structure and ELF isosurface of fcc carbon at 25 TPa. The carbon atoms are depicted in grey while the green pockets enclose the maximally localized electrons. Taken together, the positions of the carbon atoms and the maxima in the ELF form the CaF_2 structure.

nearest neighbors and is very different from those of potassium (K) [34] and sodium (Na) [33] which have much smaller c/a ratios and only 6 nearest neighbors. The lower coordination numbers of the K and Na structures arise from the interstitial electrons in these electride structures, and the near ideal c/a ratio in dhcp carbon is consistent with our conclusion that it is only a weak electride.

We find dhcp carbon to be significantly more stable than hcp below 800 TPa, although hcp is more stable at higher pressures, see Fig. 1. The c/a ratio of hcp of about 1.75 is only a little larger than the ideal value of 1.633 and the volumes at each pressure are very similar, which is reflected in the fact that the hcp and dhcp curves in Fig. 1 are nearly parallel. The greater stability of the dhcp phase may be related to the existence of two inequivalent atomic positions while all atoms are equivalent in hcp. Our calculations for dhcp show a small charge transfer of roughly 0.1 electrons from the $2c$ to the $2a$ orbits. Similar behavior has been observed in the dhcp phases of K [34] and Na [33]. The hcp phase of carbon becomes more favorable than dhcp above 800 TPa, but at these pressures bcc is the most stable phase.

The band structure and electronic density of states (eDOS) of each phase is shown in the supplemental material [27]. Although the fcc and higher pressure structures of carbon are similar to those normally adopted by archetypal simple metals at low pressures, the band structures of the carbon phases are far from free-electron like. For example, the $2s/2p$ bandwidth of fcc carbon at 50 TPa is 35% smaller than the free-electron value at the same average valence density and the lower energy $2s/2p$-derived bands have a very large effective mass [27]. One clear trend in the eDOS results is the progressive $2s \rightarrow 2p$ charge transfer; sc has a small amount of s-like eDOS at the bottom of the valence band, but in sh it is almost completely p-like. The interstitial electrons occupy the bottom of the valence band of fcc carbon. The bandwidths of the $1s$ levels increase with pressure (sc: 0.5 eV at 4 TPa; sh: 1 eV at 10 TPa; fcc: 8 eV at 50 TPa; dhcp: 53 eV at 300 TPa; bcc: 150 eV at 1 PPa). Nevertheless, at 1 PPa the top of the $1s$ band of bcc carbon is still 160 eV below the bottom of the $2s/2p$ derived bands.

In conclusion, we have used DFT methods to study carbon at pressures up to 1 PPa. Our search of the potential energy surface reinforces the current consensus that, with increasing pressure, diamond is replaced by the BC8 structure and then sc. We have proposed that sh, fcc, dhcp, and bcc phases become stable at higher pressures, which completes the zero-temperature phase diagram up to 1 PPa. We have identified the mechanism for the sc $\rightarrow$ sh transition as a soft mode phonon instability of the transverse acoustic modes at the X points of the sc structure. We find sc carbon to be thermodynamically unstable at high temperatures, and above about 5000 K the BC8 phase transforms directly into sh with increasing pressure. The fcc phase is an electride in which the carbon ions are the cations and the interstitial electrons are the anions. The equivalent ionic structure is that of CaF_2. The dominance of kinetic over potential energy at extremely high pressures leads to quite uniform $2s/2p$-derived charge densities, which favors the bcc phase. Even at 1 PPa, the most stable structure is not determined by simple notions of packing but by the quantum mechanical nature of the electrons, which may give rise to simple or complex structures.

We acknowledge financial support from EPSRC (UK) and the use of the UCL Legion High Performance Computing Facility and associated support services.

*miguel.c.martinez@ucl.ac.uk

[1] H. E. Suess and H. C. Urey, Rev. Mod. Phys. **28**, 53 (1956).
[2] T. Guillot, Annu. Rev. Earth Planet. Sci. **33**, 493 (2005).
[3] P. Brassard and G. Fontaine, Astrophys. J. **622**, 572 (2005).
[4] M. Kuchner and S. Seager (unpublished).; J. C. Bond, D. P. O'Brien, and D. S. Lauretta, Astrophys. J. **715**, 1050 (2010).
[5] N. Madhusudhan *et al.*, Nature (London) **469**, 64 (2010).
[6] M. D. Knudson, M. P. Desjarlais, and D. H. Dolan, Science **322**, 1822 (2008).
[7] J. H. Eggert *et al.*, Nature Phys. **6**, 40 (2009).
[8] D. K. Bradley *et al.*, Phys. Rev. Lett. **102**, 075503 (2009).
[9] J. Biener *et al.*, Nucl. Fusion **49**, 112001 (2009).
[10] F. Occelli, P. Loubeyre, and R. LeToullec, Nature Mater. **2**, 151 (2003).
[11] Y. Akahama and H. Kawamura, J. Phys.: Conf. Ser. **215**, 012195 (2010).
[12] M. T. Yin, Phys. Rev. B **30**, 1773 (1984).
[13] M. P. Grumbach and R. M. Martin, Phys. Rev. B **54**, 15730 (1996).
[14] A. A. Correa *et al.*, Phys. Rev. B **78**, 024101 (2008).
[15] M. T. Yin and M. L. Cohen, Phys. Rev. Lett. **50**, 2006 (1983).
[16] M. I. McMahon and R. J. Nelmes, Chem. Soc. Rev. **35**, 943 (2006).
[17] C. J. Pickard and R. J. Needs, Nature Mater. **9**, 624 (2010).
[18] C. J. Pickard and R. J. Needs, Phys. Rev. Lett. **97**, 045504 (2006).
[19] C. J. Pickard and R. J. Needs, J. Phys. Condens. Matter **23**, 053201 (2011).
[20] C. J. Pickard and R. J. Needs, Nature Phys. **3**, 473 (2007).
[21] C. J. Pickard and R. J. Needs, Phys. Rev. Lett. **102**, 146401 (2009).
[22] C. J. Pickard and R. J. Needs, J. Phys. Condens. Matter **21**, 452205 (2009).
[23] S. J. Clark *et al.*, Z. Kristallogr. **220**, 567 (2005).
[24] J. P. Perdew, K. Burke, and M. Ernzerhof, Phys. Rev. Lett. **77**, 3865 (1996).
[25] D. Vanderbilt, Phys. Rev. B **41**, 7892 (1990).

[26] The ratio of the volume per atom of diamond at zero pressure to that of the bcc phase at 1 PPa is about 50.
[27] See Supplemental Material at http://link.aps.org/supplemental/10.1103/PhysRevLett.108.045704 for details of the band structures and lattice dynamics.
[28] J. Sun, D. D. Klug, and R. Martonák, J. Chem. Phys. **130**, 194512 (2009).
[29] A. A. Correa, S. A. Bonev, and G. Galli, Proc. Natl. Acad. Sci. U.S.A. **103**, 1204 (2006).
[30] R. M. Wentzcovitch, B. B. Karki, M. Cococcioni, and S. de Gironcoli, Phys. Rev. Lett. **92**, 018501 (2004).
[31] H. G. von Schnering and R. Nesper, Angew. Chem., Int. Ed. Engl. **26**, 1059 (1987).
[32] B. Rousseau and N. W. Ashcroft, Phys. Rev. Lett. **101**, 046407 (2008).
[33] Y. Ma *et al.*, Nature (London) **458**, 182 (2009).
[34] M. Marqués *et al.*, Phys. Rev. Lett. **103**, 115501 (2009).